UCID-17265

Lawrence Livermore Laboratory

A CRYOFORMING EVALUATION USING HIGH-PURITY NICKEL

D. E. Lord and L. F. Meisner

September 14, 1976

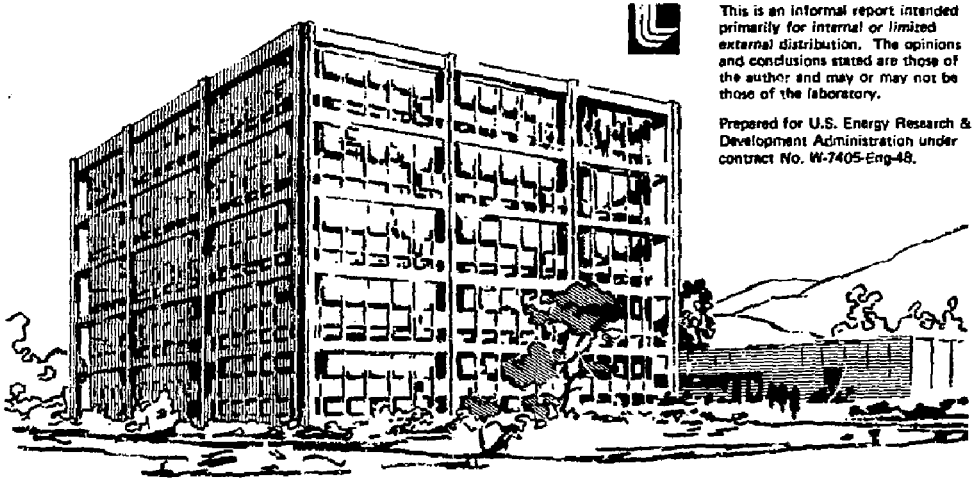

CONTENTS

A CRYOFORMING EVALUATION USING HIGH-PURITY NICKEL

ABSTRACT

We evaluated the cryogenic forming process to see if it had significant advantages over room-temperature forming. For this first in a series of evaluations, we chose a high-purity nickel (nickel 270*) because of its possible interest to Lawrence Livermore Laboratory programs. Typically, our procedure involved fast-strain-rate forming a set of nickel samples at cryogenic temperatures and another set at room temperature. We measured both sets at room temperature for failure strength, then compared their strength-preparation elongation curves at equal strains. Two more sets were formed, this time at slow strain rates (with one set at cryogenic temperatures, the other at room temperature). We measured both sets at room temperature for failure strength, then compared the strength-preparation elongation curves of these sets with the previous two at equal temperatures and strains.

Cryoforming produced a 30% higher-strength nickel than that produced at room temperature at equal strains and strain rates. Forming rate effects disappeared as working temperature decreased. Rate-insensitive cryoforming produced a considerably stronger room-temperature material than room-temperature forming at high strain rates. Transmission electron microscopy indicated apparent structural differences between cryoformed and room-temperature-formed nickel.

SOME HISTORICAL NOTES ON CRYOFORMING

Work over the last decade has centered on cryogenic forming of materials strengthened by the formation of strain martensite from an original austenitic steel structure. 301 stainless has been a favorite material for this purpose. It has produced aged room-temperature (RT) ultimate strengths of 2068 MPa (300 ksi) and static plain strain fracture toughness (K_{ic}) values of 1100 MPa $\cdot \sqrt{cm}$ (100 ksi $\cdot \sqrt{in.}$) with prestrains of less than 13%. The literature contains a number of references[1-10] on this general subject but very few on materials that do not exhibit such a phase transformation. Almost no mention

can be found of those materials whose only strengthening mechanism is cold work.

Gulyaev and Afonina[10] published results in 1970 on austenitic stainless steels (wires) with and without strain-martensite formation. Those with large percentages (95%) of strain martensite produced RT ultimate strengths of 3241 MPa (470 ksi) with cryogenic drawing (-196°C) and 2944 MPa (427 ksi) with RT drawing (20°C).

A stainless steel with zero-strain martensite (higher nickel) and comparable deformation (95%) produced strengths of 2503 MPa (363 ksi) with cryogenic drawing and 2206 MPa (320 ksi) with RT drawing.

A deformation of 60% produced 1620 MPa (235 ksi) at -196°C working temperature and 1358 MPa (197 ksi) at 20°C working temperature in a stainless steel with zero strain martensite formation.

These Gulyaev and Afonina results had original strength values of 690 MPa (100 ksi).

We found other mentions of Russian activity in this area of cryogenic forming. These mostly involve rolling and extrusion apparatus for studying strengthening mechanisms and materials properties in the superconducting state.[11,12] The Russians mention copper as a product of rolling at 77 K to 0.03 mm thickness.

Kaufman and Wanderer[13] published results in 1972 that show, in general, that aluminum alloys

7178	7075
2024	5052
5038	5082
5456	5182
6061	5557

do not respond significantly to cryoforming over room-temperature-forming. Specimens were tensile types cut from "bulged" sheet stock and standard 1/2-in. diameter tensile specimens. All strength testing was done at room temperature.

Masteller, Brown, Herzog, and Osgood[6] reported in 1970 that only two of 15 alloys showed significantly improved properties for cryoforming over RT straining. These two, PH 14-8 Mo steel and MP 35N cobalt-nickel, were strengthened by cryogenically-enhanced phase transformation. The other

materials tested were 2219 aluminum, 5456 aluminum, 6061 aluminum, beryllium copper, L605 cobalt, LA141A magnesium, Inconel 718, nickel 440, A-286 steel, TRIP steel, 21-6-9 steel, 6 Al 4v ELI titanium, and 5 Al-2.55 ELI titanium. All specimens were flat-strip tensile types tested at room temperature. The authors concluded that light microscopy could not adequately distinguish significant differences in microstructure.

Is there then any advantage in cryogenically forming materials that lack a phase transformation? Let's look again at the little positive data available, namely the work of Golvaev and Afonina[10] with wire drawing of stainless steel having no martensitic transformation:

Deformation, %	Drawing temp, °C	Ultimate strength, MPa (ksi)	Increase, %
95	-196	2503 (363)	13..
95	20	2206 (320)	
60	-196	1620 (235)	19.9
60	20	1351 (196)	

They give no information on loss of ductility. Deformation rate is given as a drawing speed of 15 m/min at -196°C. Basically, drawing is a high-rate deformation process.

So, we may conclude that cryoforming does enhance RT properties over RT-forming of the same amount of deformation. In this case, it was accomplished at high rates of deformation.

A DISCUSSION OF COLD WORKING AND CRYOGENIC STRENGTHENING

Cold working deforms a material plastically at a temperature lower than its recrystallization temperature (p. 134 of Ref. 14). This plastic deformation can also be described as strain hardening, which impedes the motion of dislocations by other dislocations (p. 189 of Ref. 14). The purpose of cold working is to enhance the strength of a material while retaining as many of its other desirable properties as possible. As part of the deformation process, subgrains form within the original structure.

F. N. Rhines,[15] in discussing hot working, ties subgrain boundary adjustment to deformation (the subgrain boundaries become more distinct as deformation proceeds). He further states that "subgrain shrinkage implies that new

subgrain boundaries can be developed during continued deformation at an increased rate, or at a reduced temperature. This is, of course, a division process and involves nucleation of new boundary, but not nucleation of new crystals."

The original grain structure of a cold-worked metal is subdivided by the formation of new boundaries composed of dislocation "tangles" (Fig. 1). The subgrains (cells) increase in number and decrease in size as the cell walls are created and increase in width. Dieter says "the formation of subgrains in an annealed material results in a significant increase in strength."[16] Strength of the cold-worked material is an inverse function of subgrain size (Fig. 2).

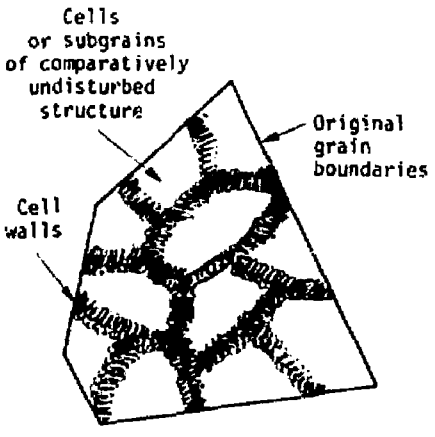

Fig. 1. Structure of a cold-worked metal.

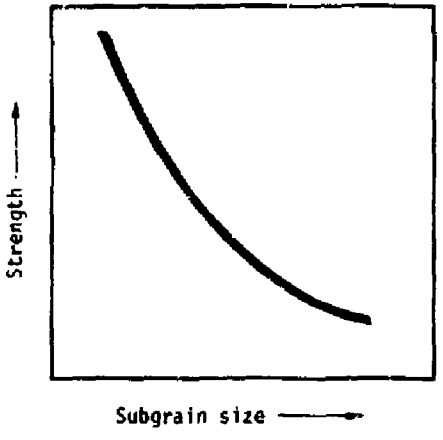

Fig. 2. Strength of cold-worked metal as a function of subgrain size.

It has long been known that, by the cold working process, strength is gained at the expense of ductility. How bad is the trade-off? Quite severe. For example, low-carbon steel can double its strength but lose 80 to 90% of its original ductility. Present design practice, however, has learned to cope with the lower ductilities of modern high-strength materials.

Wellinger and Seufert, as referenced by Brown, Herzog, Masteller, and Osgood,[6] reached the conclusion that face-centered cubic (fcc) metals and alloys

respond to cryostraining while body-centered cubic (bcc) types do not. They believe this behavior agrees with the dislocation theory of strain hardening.

Ripling, also referenced by Brown, Herzog, Masteller, and Osgood,[6] observed a ductility deficiency when straining other than fcc structures at low temperatures.

Most investigators have noted the increased capability for plastic deformation without necking (homogeneous deformation) at temperatures below room temperature.

PROCESS EVALUATION PLAN

We set out to investigate the cryogenic work behavior of materials of interest to us. Specifically, we looked at the effects of

- forming temperature,
- forming rate, and
- post-forming heat treatment (if possible)

on

- ultimate strength and
- ductility (elongation).

We asked these basic questions:

- Are there significant advantages to cryoforming over RT forming?
- Are there significant advantages to high-rate forming over slow-rate forming?
- In the case of significant strengthening, is it possible to correlate strength with the microstructure by transmission electron microscopy (TEM)?

Often the prime reason for a material choice is not strength alone. Electrical, chemical, or neutronic properties or other special behavior may be first in importance. In some instances, the first consideration can be reasonably satisfied (along with strength-size limitations) by choice of an alloy. In others, the prime factors so outweigh all other considerations that a material is "the only one." Now our problem is to arrive at a reasonable strength to minimize size and weight. Many of these special purpose materials are those whose only strengthening mechanism is cold work.

We chose material on the basis of possible interest to Lawrence Livermore Laboratory programs. Nickel 270 has possible use as a substrate for physically

weak superconducting materials. This material has an fcc structure. It is the first in an intended series of materials to be evaluated.

At the time, the most direct approach seemed to be that of uniaxial specimens prestrained at various temperatures and rates. We also looked at other temperature low-rate strengths of the nickel because of its intended use range.

APPARATUS

High-rate forming required special apparatus (Fig. 3). We accomplished medium- and slow-rate forming and all other testing with conventional test machines and extensometry.

A traveling-stage optical system was used to make gage-length and specimen dimensional measurements.

TYPICAL TEST PROCEDURE

1. Check dimensions and scribe gage marks on specimens.
2. Optically measure gage length and cross section.
3. Use high-rate machine or conventional test machine for prestraining.
4. Optically measure prestrain and new cross section.
5. Test to failure in conventional manner with extensometer strain measurement.
6. Make final optical strain measurement.

SPECIMEN CONFIGURATION AND COMPOSITION

The nickel 270 specimens were cut from 1.42-mm (0.056-in.) sheet stock according to a sampling plan designed to avoid directional property differences. Figure 4 shows the specimen configuration (Tab 02 gives the specimen size). It has a 25.4-mm (1-in.) gage length by a 6.35-mm (0.250-in.) width and pin-type grip ends.

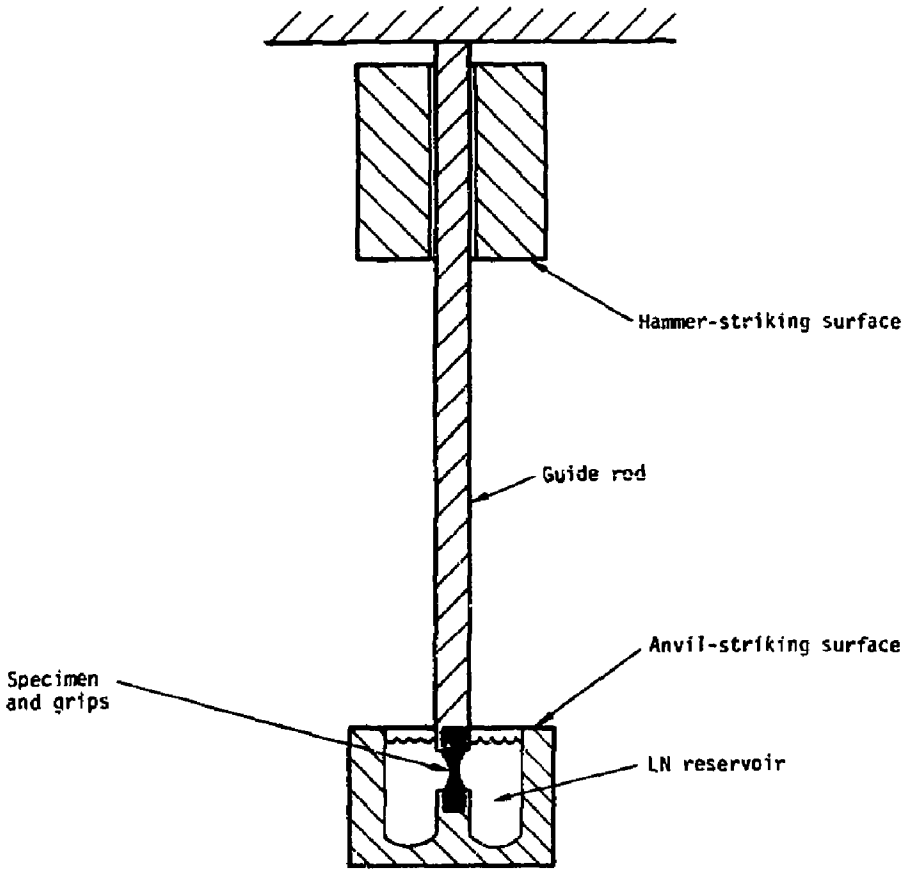

Fig. 3. Apparatus for high-rate forming (straining).

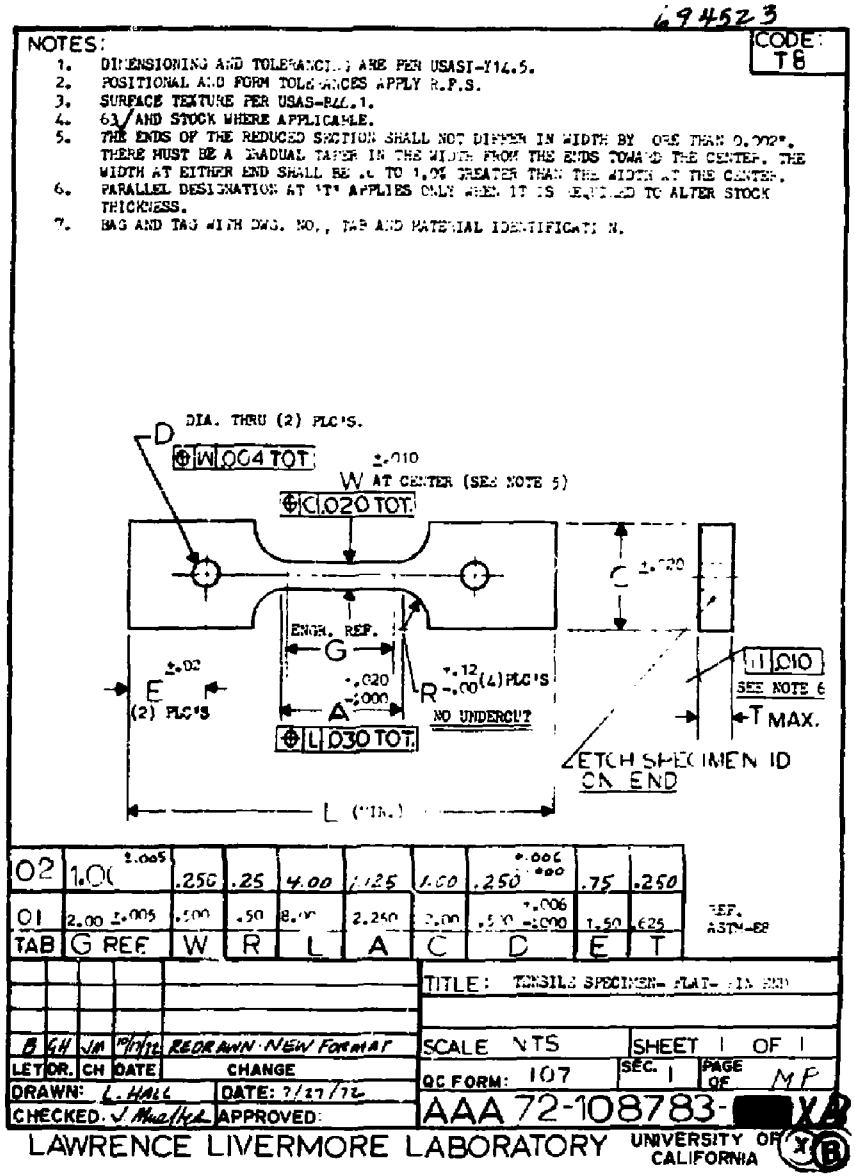

Fig. 4. Tensile specimen configuration.

Nickel 270, a high-purity material, has the following chemical composition:[17]

Element	Wt%
	Min
Nickel	99.97
	Max
Copper	0.001
Iron	0.005
Manganese	0.001
Carbon	0.02
Silicon	0.001
Sulfur	0.001
Cobalt	0.001
Chromium	0.001
Magnesium	0.001
Titanium	0.001

FORMING AND TESTING CONDITIONS

These are the strain rates and temperatures for both prestraining and testing:

Prestrain rates

Fast	10^{2}/sec
Medium	10^{0}/sec
Slow	10^{-4}/sec, 10^{-2}/sec

Test rate

Slow	10^{-4}/sec

Prestrain temperatures (°C)

Liquid nitrogen (LN)	-196
Room temperature	24

Test temperatures (°C)	
Liquid helium (LHe)	-269
Liquid nitrogen	-196
Dry ice and acetone	-84
Room temperature	24
Test furnace	300

MICROSTRUCTURE COMPARISONS

We attempted to compare microstructures using TEM techniques. Previous investigators[6] indicated light microscopy was not adequate for this purpose. We also "tracked" the deformation process using this technique.

The first series of TEM pictures (Fig. 5) shows the changes as the annealed material progressed through 6 and 30% deformations. This deformation was performed in LN.

The second series (Figs. 6 and 7) compares an LN-prepared 30%-deformed material with a RT-prepared, 30%-deformed material.

There is a distinct difference between the structures. The cryoformed material seems to show distributed dislocation arrays within the cell itself. The RT-formed material exhibits much less of this (the cells appearing relatively undisturbed like the original material). The cell sizes in the cryoformed material also tend to be somewhat smaller than those of the RT-formed material.

RESULTS

The appendix contains the detailed test results for all nickel 270 samples. Our evaluation revealed that cryoforming produced a 30% stronger material than RT-forming when comparing slow prestraining rates at 40% deformation. We produced a 20% stronger material when comparing fast prestraining rates at the same deformation (Fig. 8).

On a strain energy input basis (area under stress-strain curve), the differences are similar (Fig. 9).

At LN-forming temperature, the difference between the slow and fast prestraining rates appears to disappear (Fig. 10).

Figure 11 shows ductility loss and ultimate strengths of LN-prepared material at several testing temperatures.

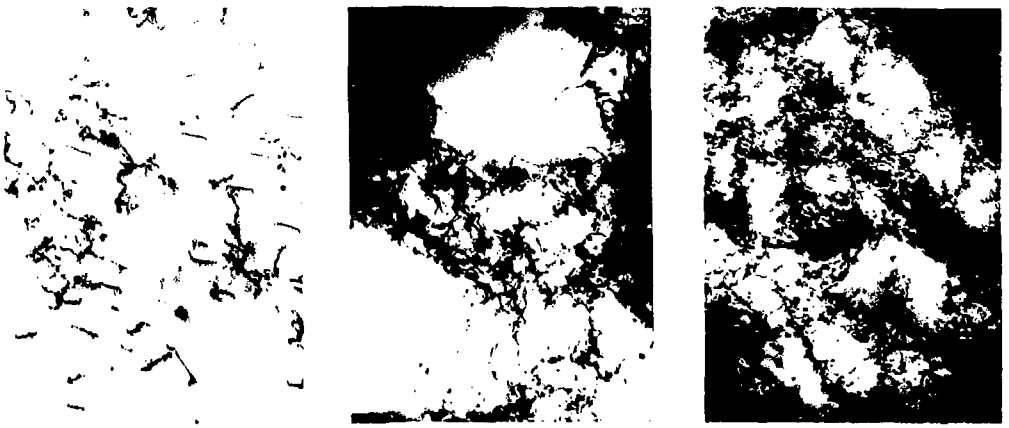

Fig. 5. Deformation (%) sequence for nickel 270 (left to right: 0%, 6%, 30%). TEM magnification = 50 000X.

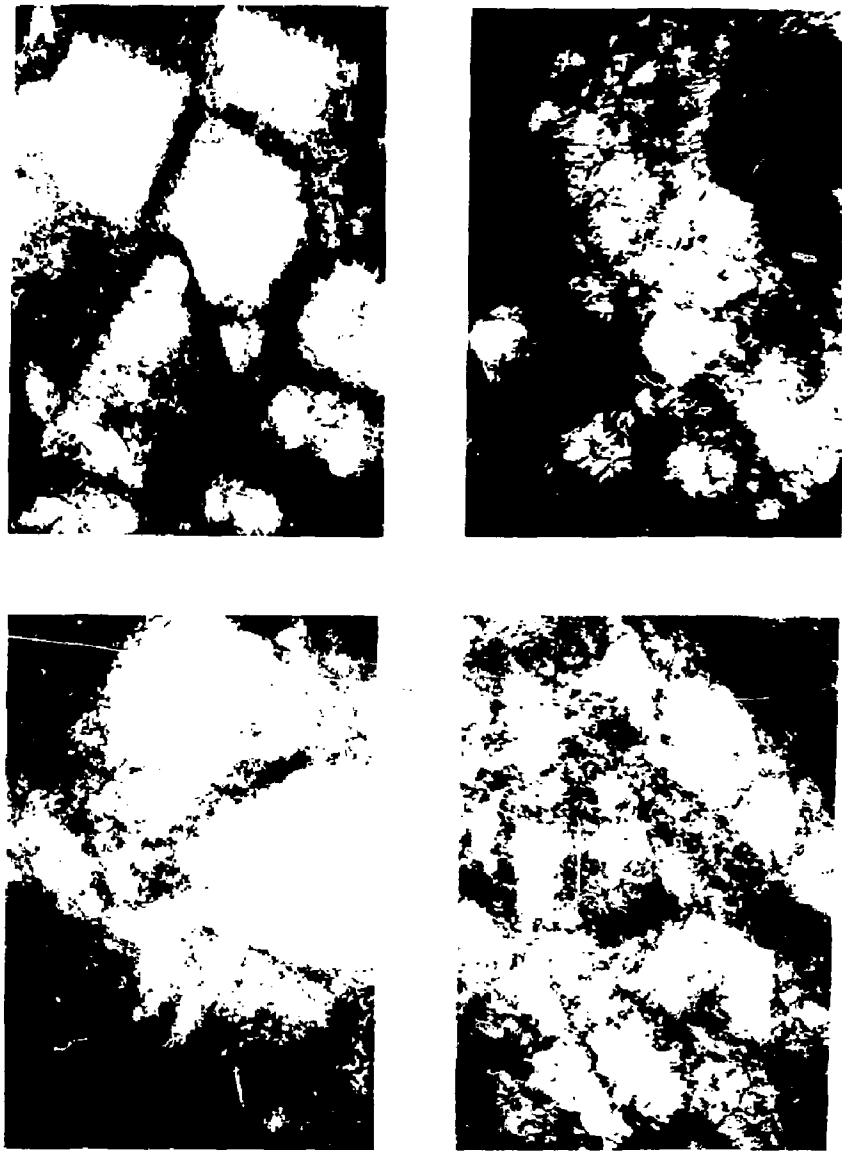

Fig. 6. TEM comparison of RT vs LN-worked nickel 270: RT (left); LN (right). Deformation = 30% (all cases). At 33 000X (top) and 50 000X (bottom).

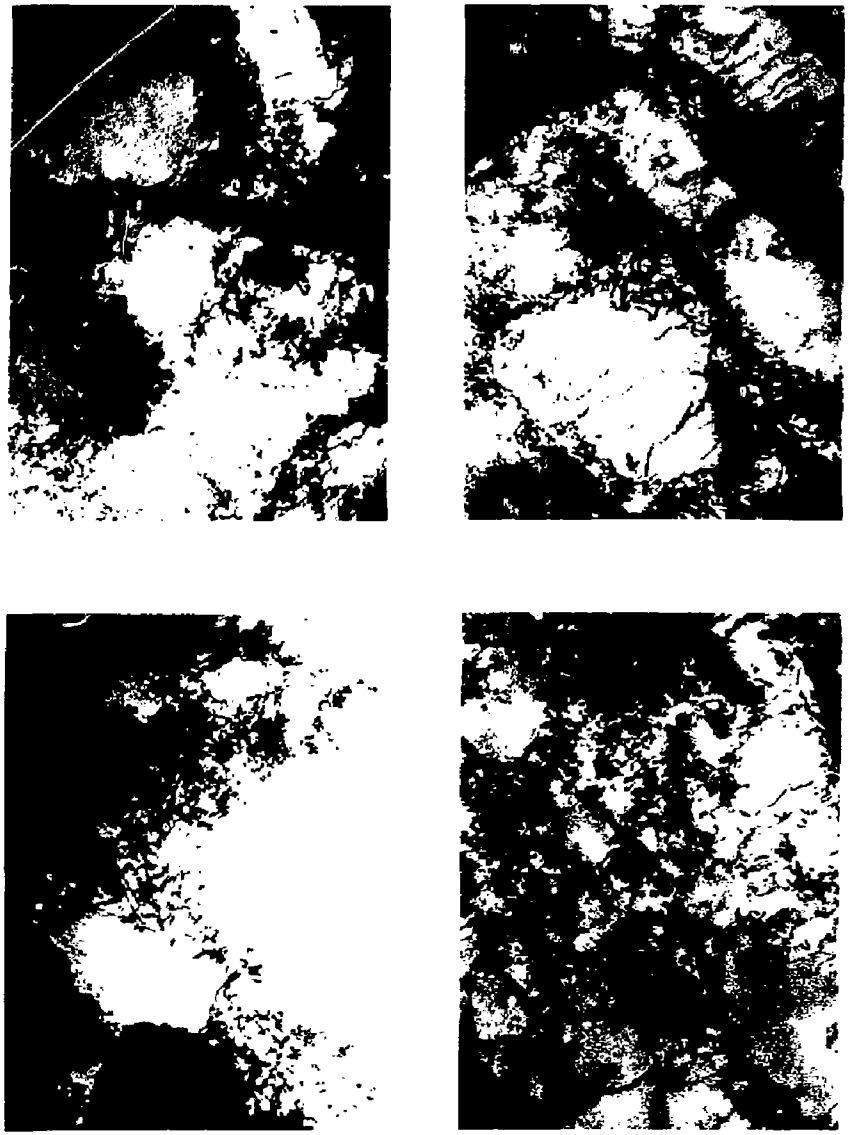

Fig. 7. TEM comparison of RT vs LN-worked nickel 270: RT (left); LN (right). Deformation = 30% (all cases). At 50 000X (top) and 67 000X (bottom).

Figures 12 to 14 show typical plastic behavior for 20%, 30%, and 50% LN-prestrained material tested at various temperatures.

Since nickel "avalanche" anneals, no improvement in ductility could be made by subsequent heat treating. Nickel either remains in its worked condition or is annealed.

As previous investigators have found, the limit of homogeneous deformation is much greater with cryoformed material than with RT-formed material. The limit at RT is about 40% while the limit at LN exceeds 50% without necking. Fast-rate straining improves the RT homogeneous limit at RT.

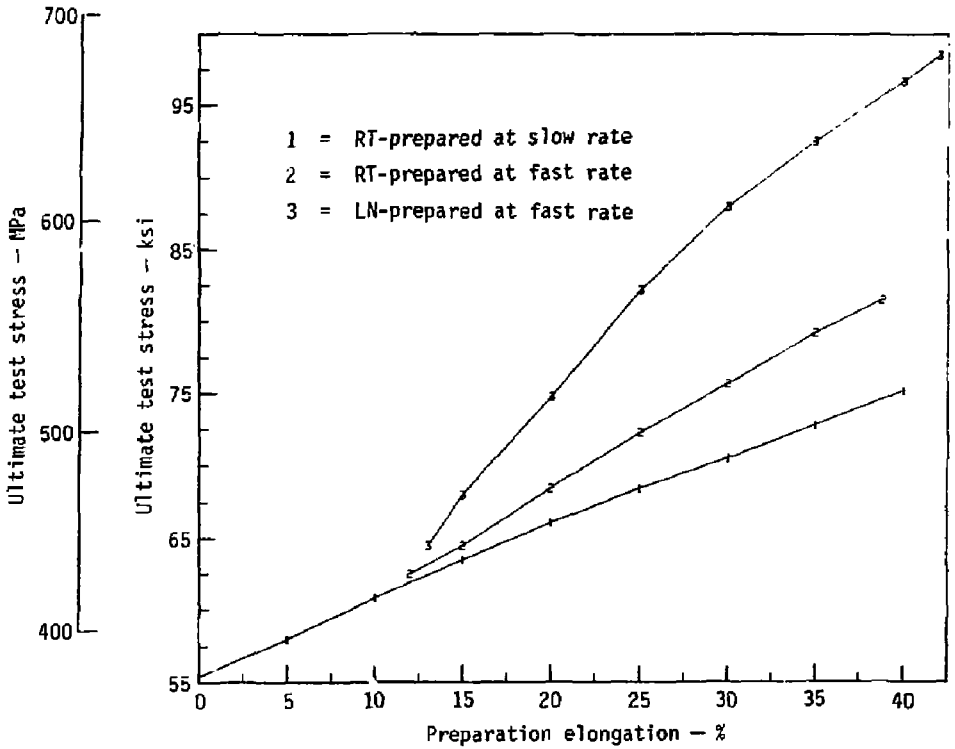

Fig. 8. These nickel 270 curves show the added strength derived from high-rate forming over low-rate at RT. They also show the added strength gained from cryoforming over RT-forming.

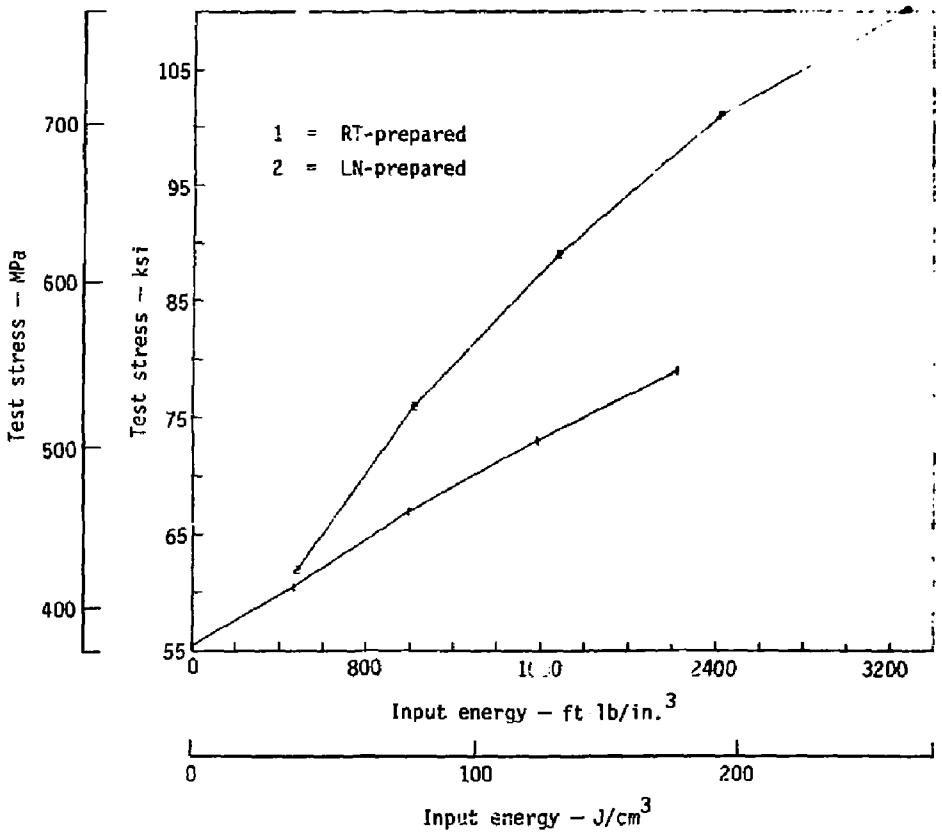

Fig. 9. Slow-rate curves (prestrained at LN and RT) as a function of input strain energy. These curves show the ability of cryoformed material to absorb strain energy in a homogeneous fashion and produce a higher-strength material.

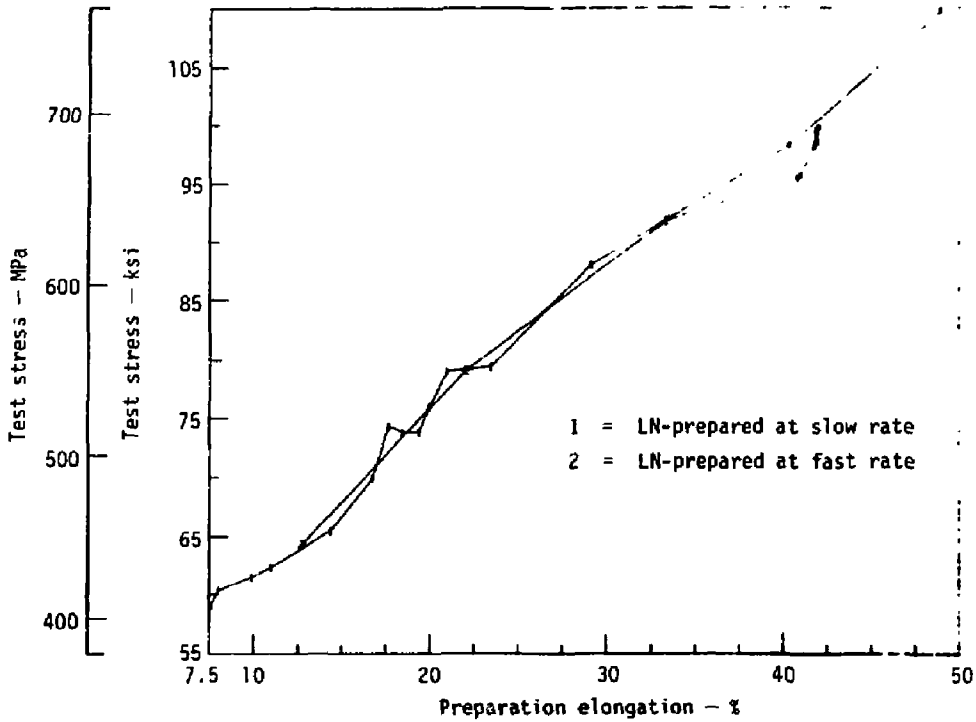

Fig. 10. These slow- and fast-rate curves show virtually no difference between prestrain rates at LN temperatures.

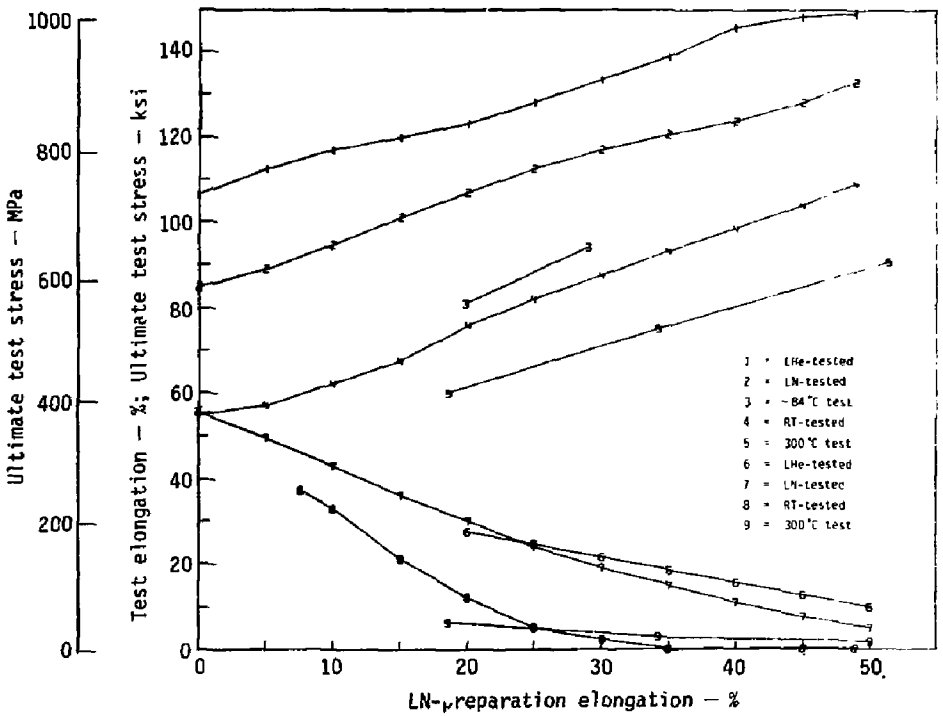

Fig. 11. The top (ascending) group of curves shows the strengths obtained by testing at various temperatures. The bottom (descending) group shows the corresponding loss of ductility. Both are plotted against preparation elongation (prestrain). We prepared the nickel at LN temperature and slow strain rate.

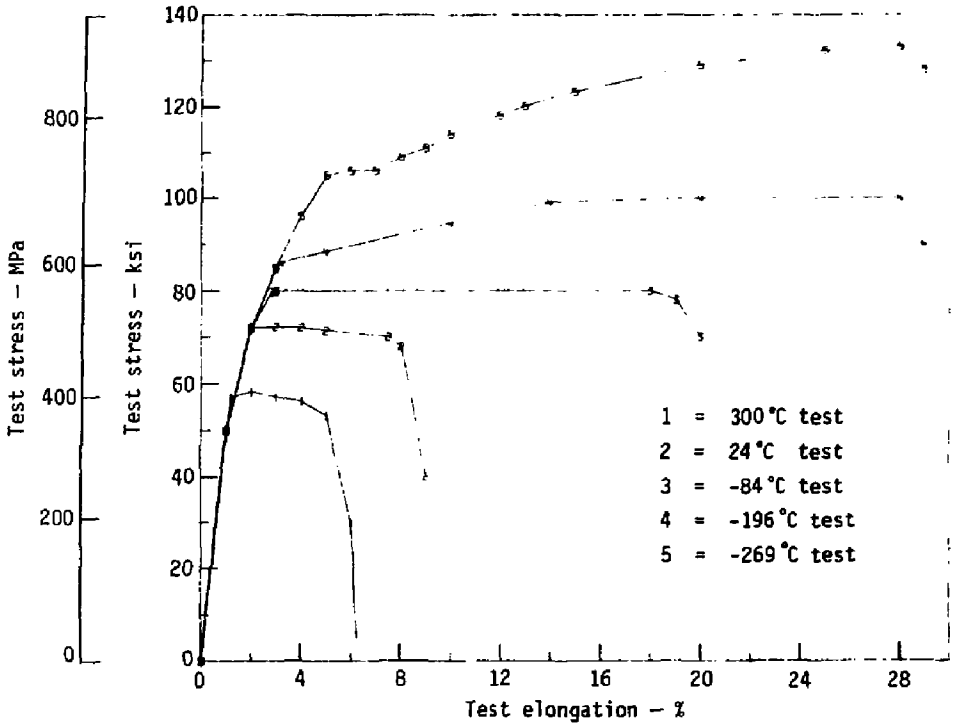

Fig. 12. Plastic behavior of LN-prepared nickel tested to 20% elongation at different temperatures and a slow strain rate. Note the evident ductility decrease and strength increase.

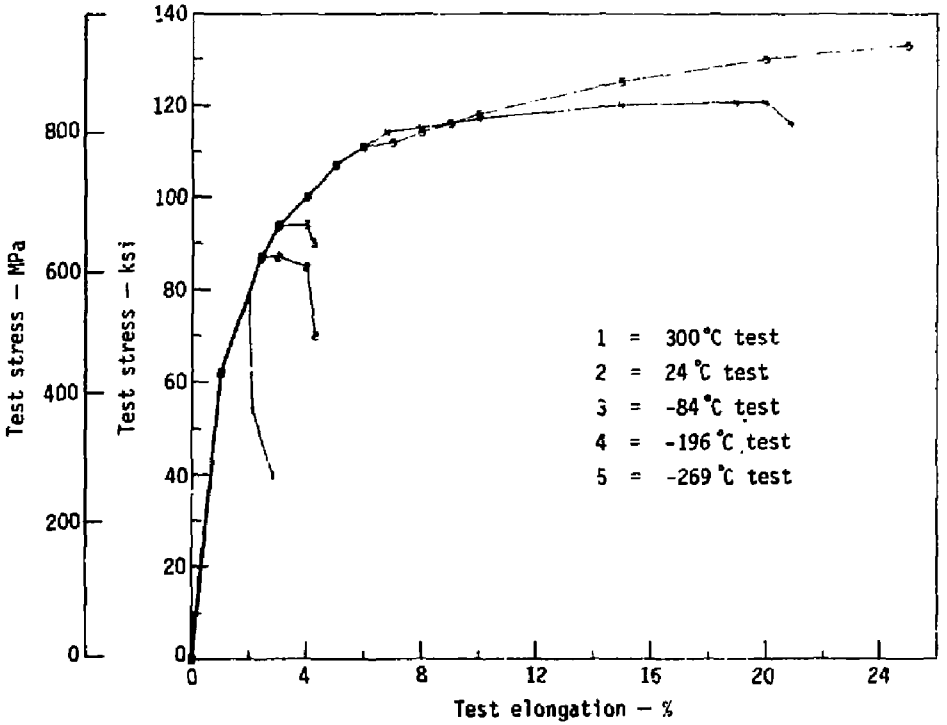

Fig. 13. Plastic behavior of LN-prepared nickel tested to 30% elongation. See Fig. 12 caption for comments.

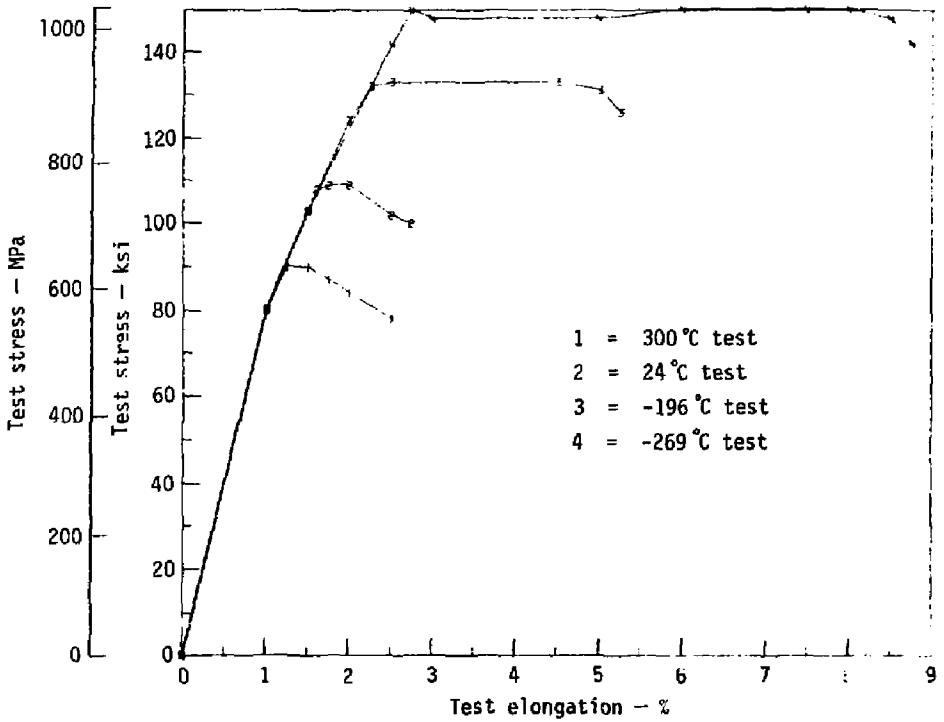

Fig. 14. Plastic behavior of LN-prepared nickel tested to 50% elongation. See Fig. 12 caption for comments.

CONCLUSIONS

Based on the nickel results:

- Cryoforming has significant advantages over RT-forming.
- Cryoforming produces a considerably stronger material at RT than RT-forming at high strain rates.
- Cryoforming allows for a greater homogeneous deformation at cryotemperatures than is possible even at fast rates at RT.
- Forming rate effects at cryotemperature appear to be completely insignificant as far as strength is concerned.
- There appear to be structural differences between cryoformed and RT-formed material as seen in the TEM comparisons.

FUTURE WORK

If sufficient interest can be generated, we would like to pursue some biaxial cryoforming and testing. This is a much better test than with uniaxial specimens because of the instabilities inherent in some materials under uniaxial loading.

ACKNOWLEDGMENTS

We thank R.G. Stone for support of this project under the auspices of the Engineering Research Program. Leo Meisner led the program operations, including data reduction. Jim Kuhlman did most of the high rate deformation and was responsible for all such fixturing. Thanks are also due Bob Brady and Rich Cortez for their contributions to the testing program. The scanning electron microscope work was done by Sam Digiallonardo.

Professor Amiya Mukherjee was very helpful during the course of the investigation.

REFERENCES

1. A.G. Imgram, *Cryogenic Forming of Type 301 Stainless Steel*, Battelle Mem. Inst., Columbus, Ohio, Rept. RSIC-408 (1965).

2. D.L. Daigle, *Evaluation of Three Arde-Portland Cryogenic Stretched Formed Subscale Rocket Motor Cases*, Thiokol Chemical Corp., Huntsville, Alabama, Rept. U-65-21A, 21-65 (1965).

3. T.W. Orange, *Evaluation of Special 301-Type Stainless Steel for Improved Low Temperature Notch Toughness of Cryoformed Pressure Vessels*, NASA, Lewis Research Center, Cleveland, Ohio, Rept. TN-D-3445 (1966).

4. A. Cozewith, *Metal Progress* 96 (1), 64 (1969).

5. C.N. Irvine, *Cryoformed 301 Stainless Steel for Pressure Vessels*, NASA, Huntsville, Alabama, Rept. TMX-53978 (1969).

6. H.J. Brown, R.G. Herzog, R.D. Masteller, and S.H. Osgood, *Properties of Cryogenically Worked Materials, Interim Report*, NASA, Lewis Research Center, Cleveland, Ohio, Rept. CR-72638 (1970).

7. D. Gleich, *Development of a Filament-Overwrapped Cryoformed Metal Pressure Vessel Final Report, July 1967-August 1970*, NASA, Lewis Research Center, Cleveland, Ohio, Rept. CR-72753/Arde 41001 (1971).

8. D. Gleich, *Space Shuttle Materials* 3, 527 (1971).

9. D.A. Prokoshkin, A.G. Galov, A.G. Vasil'eva, A.S. Belousov, and V.N. Gubanova, *Metallovedenie i Term. Obrabot. Metallov* 11, 11 (1971).

10. A.P. Gulyaev and V.M. Afonina, *Metallovedenie i Term. Obrabot. Metallov* 11, 5 (1971).

11. I.A. Ginden, S.F. Kravchenko, and Ya. D. Starodubov, *Prilory i Tekhn. Eksper.* 6, 206 (1970).

12. I.A. Ginden, S.F. Kravchenko, Ya. D. Starodubov, and V.M. Matsevity, *Prilory i Tekhn. Eksper* 6, 207 (1970).

13. J.G. Kaufman and E.T. Wanderer, "The Tensile Properties of Aluminum Alloys Formed at Cryogenic Temperatures," in *Advances in Cryogenic Engineering, Vol 18* (Plenum Press, New York-London, 1973).

14. A.S. Tetelman and A.J. McEvily, Jr., *Fracture of Structural Materials* (John Wiley & Sons, Inc., New York-London-Sydney, 1967), pp. 188-189.

15. F.N. Rhines, "Evolution of Microstructure During Hot Plastic Deformation," in *The Inhomogeneity of Plastic Deformation* (American Society for Metals, Metals Park, Ohio, 1973).

16. G.E. Dieter, Jr., *Mechanical Metallurgy* (McGraw-Hill, New York-Toronto-London, 1961), p. 127.

17. *Huntington Nickel Alloy Bulletin* (International Nickel Co., Huntington, West Virginia, 1972), 2nd ed.

LG/gw/vt/gw

APPENDIX

TEST RESULTS FOR NICKEL 270 SAMPLES

Table 1. Test results for samples of nickel 270.

Sample	Cold working			Testing			
	Temp, °C	Strain rate	Elong., %	Temp, °C	Strain rate	Elong., %	Ultimate stress, MPa (ksi)
A1B	-196	10^{-4}	7.6	24	10^{-4}	37.4	407.5 (59.1)
A2B			8.0			36.3	416.4 (60.4)
A4B			9.9			32.7	424.0 (61.5)
A3B			11.0			29.7	429.5 (62.3)
A1C			14.4			23.5	451.6 (65.5)
A2C			16.8			17.9	481.9 (69.9)
A4E			19.4			9.0	508.8 (73.8)
2089			17.7			12.4	512.3 (74.3)
2090			18.5			12.1	508.8 (73.8)
2086			20.0			10.0	534.3 (77.5)
2087			20.0			9.2	518.5 (75.2)
2088			20.0			10.6	517.0 (75.0)
2085			21.0			8.0	542.6 (78.7)
2100			21.0			6.9	547.4 (79.4)
793			23.5			5.5	547.4 (79.4)
B2A			29.2			4.5	606.7 (88.0)
764			40.4			1.0	677.1 (98.2)
B1D		10^{-4}	48.9			2.8	755.7 (109.6)
789		10	11.0			31.4	424.0 (61.5)
768			16.3			13.7	476.4 (69.1)
794			19.8			5.5	515.7 (74.8)
790			26.0			4.9	590.9 (85.7)
775			29.9			4.9	627.4 (91.0)
796		1.0	36.4			3.0	664.0 (96.3)
778		10^{2}	12.8			28.0	443.3 (64.3)
783			22.1			6.0	545.4 (79.1)
770			33.5			—	632.9 (91.8)
786			41.0			2.2	658.4 (95.5)
780			41.9			2.3	677.8 (98.3)
773	-196	10^{2}	42.0	24	10^{-4}	0.1	686.7 (99.6)

Table 1. Continued.

Sample	Cold working: Temp, °C	Cold working: Strain rate	Cold working: Elong., %	Testing: Temp, °C	Testing: Strain rate	Testing: Elong., %	Testing: Ultimate stress, MPa (ksi)
797	24	10^{-4}	0	24	10^{-4}	52.1	381.3 (55.3)
791	↑	↑	0	↑	↑	50.9	382.7 (55.5)
784	↑	↑	21.6	↑	↑	27.5	461.3 (66.9)
797'	↑	↓	29.6	↑	↑	17.3	485.4 (70.4)
792	↑	10^{-4}	40.2	↑	↑	7.7	518.5 (75.2)
767	↑	10^{0}	18.9	↑	↑	20.7	452.3 (65.6)
765	↑	10^{0}	36.2	↑	↑	5.3	537.1 (77.9)
777	↑	10^{2}	11.5	↑	↑	36.0	426.8 (61.9)
774	↑	↑	21.5	↑	↑	18.7	479.2 (69.5)
779	↑	↑	30.0	↑	↑	6.5	522.6 (75.8)
766	↑	↑	38.7	↑	↑	4.1	561.9 (81.5)
782	↑	↓	40.8	↑	↑	4.0	558.5 (81.0)
781	↑	10^{2}	44.5	24	↑	6.0	561.9 (81.5)
B1C	↑	10^{-4}	22.2	-196	↑	24.3	448.2 (65.0)
B3C	24	↑	19.9	-196	↑	24.9	447.5 (64.9)
787	-196	↑	39.0[a]	24	↑	40.5	359.9 (52.2)
754	↑	↑	39.5[b]	↑	↑	8.8	426.8 (61.9)
755	↑	↑	39.7[a]	↑	↑	43.6	377.8 (54.8)
788	↓	↓	40.3[c]	↓	↑	2.3	675.7 (98.0)
769	-196	10^{-4}	40.3[d]	24	10^{-4}	2.0	661.2 (95.9)
B4B	-196	10^{-4}	0	-196	10^{-4}	54.4	581.9 (84.4)
B3B	↑	↑	0	↑	↑	54.0	606.7 (88.0)
B3F	↑	↑	0	↑	↑	56.0	608.1 (88.2)
B2C	↑	↑	19.0	↑	↑	17.2	482.6 (70.0)
A3E	↑	↑	19.6	↑	↑	29.2	702.6 (101.9)
2099	↑	↑	20.1	↑	↑	21.7	709.5 (102.9)
A3C	↑	↑	23.0	↑	↑	26.6	792.2 (114.9)
B1A	↑	↑	28.2	↑	↑	20.8	833.6 (120.9)
A4C	↓	↓	29.4	↓	↑	20.2	760.5 (110.3)
B1E	-196	10^{-4}	48.5	-196	10^{-4}	5.7	913.6 (132.5)

Table 1. Continued.

Sample	Cold working			Testing			
	Temp, °C	Strain rate	Elong., %	Temp. °C	Strain rate	Elong., %	Ultimate stress, MPa (ksi)
B4D	-196	10^{-4}	49.3	-196	10^{-4}	4.4	919.1 (133.3)
B4F	↑	↑	0	-269	↑	47.5	735.0 (106.6)
A4D	↑	↑	19.8	↑	↑	27.4	848.1 (123.0)
A3D	↑	↑	20.0	↑	↑	26.0	792.2 (114.9)
2098	↑	↑	20.1	↑	↑	28.1	857.0 (124.3)
A2F	↑	↑	20.5	↑	↑	29.0	917.0 (133.0)
B2B	↑	↑	28.5	↑	↑	18.8	894.3 (129.7)
B1B	↑	↑	28.7	↑	↑	25.0	917.0 (133.0)
B3D	↑	↑	48.6	↑	↑	11.0	1041.1 (151.0)
B3E	↑	↑	49.2	↑	↑	12.0	1034.2 (150.0)
B4E	↑	10^{-4}	49.6	↑	↑	8.8	1041.1 (151.0)
B1F	↑	10^{-2}	49.8	↓	↑	6.2	1006.6 (146.0)
B2F	↑	10^{-2}	50.9	-269	↑	3.4	1034.2 (150.0)
A1D	↑	10^{-4}	19.8	-84	↑	21.5	557.8 (80.9)
A2D	↑	↑	19.6	↑	↑	20.8	559.9 (81.2)
B3A	↑	↑	29.0	↓	↑	4.5	648.1 (94.0)
A1E	↑	↑	18.6	-84	↑	6.4	408.2 (59.2)
A2E	↑	↑	18.4	300	↑	6.2	424.0 (61.5)
B4A	↑	↑	34.2	↑	↑	3.0	546.1 (79.2)
B2D	↑	↑	51.4	↓	↑	2.1	624.0 (90.5)
B2E	-196	10^{-4}	46.8	300	10^{-4}	2.8	633.6 (91.9)

[a]Annealed at 482°C.

[b]Annealed at 427°C.

[c]Annealed at 316°C

[d]Annealed at 371°C.

Printed in the United States of America
Available from
National Technical Information Service
U.S. Department of Commerce
5285 Port Royal Road
Springfield, VA 22161
Price: Printed Copy $; Microfiche $2.25

Page Range	Domestic Price	Page Range	Domestic Price
001–025	$ 3.50	326–350	10.00
026–050	4.00	351–375	10.50
051–075	4.50	376–400	10.75
076–100	5.00	401–425	11.00
101–125	5.50	426–450	11.75
126–150	6.00	451–475	12.00
151–175	6.75	476–500	12.50
176–200	7.50	501–525	12.75
201–225	7.75	526–550	13.00
226–250	8.00	551–575	13.50
251–275	9.00	576–600	13.75
276–300	9.25	601–up	*
301–325	9.75		

*Add $2.50 for each additional 100 page increment from 601 to 1,000 pages; add $4.50 for each additional 100 page increment over 1,000 pages.